NIH Public Access
Author Manuscript
J Neurochem. Author manuscript; available in PMC 2013 September 01.

Published in final edited form as:
J Neurochem. 2012 September ; 122(6): 1145–1154. doi:10.1111/j.1471-4159.2012.07839.x.

Thermal sensitivity of voltage-gated Na^+ channels and A-type K^+ channels contributes to somatosensory neuron excitability at cooling temperatures

Ignacio Sarria, **Jennifer Ling**, and **Jianguo G. Gu**
Department of Anesthesiology and the Graduate Program in Neuroscience, The University of Cincinnati College of Medicine, PO Box 670531, 231 Albert Sabin Way, Cincinnati, OH 45267

Abstract

Cooling temperatures may modify action potential firing properties to alter sensory modalities. Here we investigated how cooling temperatures modify action potential firing properties in two groups of rat dorsal root ganglion (DRG) neurons, tetrodotoxin-sensitive (TTXs) Na^+ channel-expressing neurons and tetrodotoxin-resistant (TTXr) Na^+ channel-expressing neurons. We found that multiple action potential firing in response to membrane depolarization was suppressed in TTXs neurons but maintained or facilitated in TTXr neurons at cooling temperatures. We showed that cooling temperatures strongly inhibited A-type K^+ currents (IA) and TTXs Na^+ channels but had fewer inhibitory effects on TTXr Na^+ channels and non-inactivating K^+ currents (IK). We demonstrated that the sensitivity of A-type K^+ channels and voltage-gated Na^+ channels to cooling temperatures and their interplay determine somatosensory neuron excitability at cooling temperatures. Our results provide a putative mechanism by which cooling temperatures modify different sensory modalities including pain.

Keywords

Cold; voltage-gated Na^+ channels; voltage-gated K^+ channels; dorsal root ganglions; pain

Introduction

Cooling temperatures from 30 °C to ~15 °C are innocuous but below ~15 °C provoke painful sensations (Morin & Bushnell 1998). Cooling temperatures also affect other sensory modalities including touch (Phillips & Matthews 1993), itch (Fruhstorfer et al 1986) and pain (Meeusen & Lievens 1986). For example, touch sensations become less acute and itch can be relieved at cooling temperatures (Fruhstorfer et al 1986; Phillips & Matthews 1993). More interestingly, acute pain such as ankle sprain can be relieved (Meeusen & Lievens 1986) but chronic arthritic pain and neuropathic can become exacerbated by cold temperatures (Guedj & Weinberger 1990; McAlindon et al 2007; Sato 2003; von Mackensen et al 2005). While the sense of both innocuous and noxious cold has been largely attributed to the activation of TRPM8 channels expressed on a subpopulation of primary afferents (McKemy et al 2002; Peier et al 2002), how cooling temperatures affect other sensory modalities remain to be obscure.

Correspondence and requests for the materials should be addressed to Jianguo G. Gu, M.B., Ph.D., University of Cincinnati, PO Box 670531, 231 Albert Sabin Way, Cincinnati, OH 45267-0531., Fax: (513) 558-0995, gujo@uc.edu.

The authors declare no conflict of interests.

NIH-PA Author Manuscript
NIH-PA Author Manuscript
NIH-PA Author Manuscript

NIH-PA Author Manuscript

NIH-PA Author Manuscript

NIH-PA Author Manuscript

The effects of cooling temperatures on other sensory modalities may occur at a conduction level, and is determined by action potential firing properties at cooling temperatures. Voltage-gated Na^+ channels and K^+ channels are two main determinants of action potential firing properties. Adult somatosensory neurons express several types of voltage-gated Na^+ channels (Dib-Hajj et al 2010). They can be generally classified into tetrodotoxin-sensitive (TTXs) and tetrodotoxin-resistant channels (TTXr) based on TTX block. Sensory neurons that express TTXr channels are mostly nociceptors and those that only express TTXs are mainly non-nociceptors (Akopian et al 1996; Dib-Hajj et al 2010). TTXs and TTXr channels are determinants for action potential thresholds in sensory neurons (Yoshimura et al 1996) and TTXr channels are essential for pain at low temperatures (Zimmermann et al 2007).

Voltage-gated A-type K^+ currents (IA currents) are involved in modulating the action potential shape, threshold and the inter-spike interval in sensory neurons (Yoshimura et al. 1996; Yost 1999). Several subtypes of IA currents have been identified in DRG neurons (Gold et al 1996; Rasband et al 2001; Yoshimura et al 1996). In nociceptive neurons, IA currents have been proposed to function as a brake to counteract membrane depolarization and thereby restrict nociceptive neuron excitability (Sculptoreanu et al 2004; Vydyanathan et al 2005). Down-regulation of IA currents occurred following nerve injury, contributing to an increase in nociceptive neuron excitability that leads to neuropathic pain conditions including cold allodynia (Chien et al 2007; Tan et al 2006). In the present study, we show that cooling temperatures have differential effects on TTXs and TTXr DRG neuron excitability and action potential firing properties. The cooling effects are attributed to both the inhibition of IA currents and the differential suppression of voltage-gated Na^+ channels by cooling temperatures.

Materials & Methods

Sprague Dawley rats (100–250 g, both genders) were used. Animal care and use conformed to NIH guidelines for care and use of experimental animals. Experimental protocols were approved by the University of Cincinnati Institutional Animal Care and Use Committee. DRG neuron cultures were prepared as described previously (Tsuzuki et al 2004) and maintained in MEM medium that contained 5% heat-inactivated horse serum. Cells were used within 36 hrs after plating.

Cultured neurons were continuously perfused at 2 ml/min with a normal bath containing (in mM) 150 NaCl, 5 KCl, 2 $MgCl_2$, 2 $CaCl_2$, 10 glucose, 10 HEPES, pH 7.3, osmolarity 330 mOsm, 24 °C. They were first tested with cold bath (15 °C) and 100 μM menthol to pre-identify cold/menthol-insensitive cells by using the Ca^{2+} imaging method (Sarria & Gu 2010). Recordings were performed on cold/menthol-insensitive cells to avoid the complications introduced by cold transducer activation. Recording electrode resistance after filling internal solutions (see below) was 4–6 MΩ. Junction potentials were corrected for in the data analysis. Electrophysiological signals were recorded with an Axopatch 200B amplifier, filtered at 2 kHz, and sampled at 10 kHz using pCLAMP 9.0 (Axon Instruments).

For experiments to determine action potential firing properties, electrode internal solution contained (in mM) 135 K-Gluconate, 5 KCl, 2.4 $MgCl_2$, 0.5 $CaCl_2$, 5 EGTA, 10.0 Hepes, 5.0 Na_2ATP, 0.33 GTP-Tris salt, pH 7.35 and 320 mOsm. Each cell was first tested with 500 nM TTX to determine if a cell had only TTXs Na^+ channels (TTXs cell) or had TTXr Na^+ channels (TTXr cell) as well. This was achieved under voltage-clamp configuration by recording inward currents in response to a series of voltage steps (10 mV each step, ranging from −90 to 10 mV) from a holding potential of −80 mV in the absence and presence of 500 nM TTX. The TTX-sensitivity test was performed in a bath solution that contained (in mM) 70 NaCl, 50 Choline-Cl, 1 $MgCl_2$, 0.01 $CaCl_2$, 10 glucose, 10 HEPES, pH 7.3, 330 mOsm.

NIH-PA Author Manuscript

NIH-PA Author Manuscript

NIH-PA Author Manuscript

Bath solution was then switched back to normal bath (wash for >10 min) and recordings were switched to current-clamp configuration. To determine the effect of cooling temperatures on action potential firing properties, a series of square pulse currents were injected into the cells at temperatures of 29 °C, 24 °C, 15 °C, and 10 °C. The temperatures of bath solutions were controlled by a Peltier cooling device (Warner Instrument, CT, USA).

For experiments to determine effects of cooling temperatures on voltage-gated Na^+ channels and voltage-gated K^+ channels, voltage-clamp recordings were performed at temperature of 29 °C, 24 °C, 15 °C, or 10 °C. For isolating sodium currents, the bath contained (in mM) 70 NaCl, 50 Choline-Cl, 20 TEA-Cl, 1 $MgCl_2$, 0.01 $CaCl_2$, 10 glucose, 10 HEPES, pH 7.3 and 330 mOsm. Electrode internal solution was similar to the above for action potentials except K^+ was replaced with Cs^+. Isolated Na^+ currents were activated by test pulses to 10 mV (TTXs) or 0 mV (TTXr) from holding potentials (Vh) of −120 mV or −80 mV, respectively. For steady-state fast inactivation, 50-ms pre-pulses from −140 mV (TTXs) or −120 mV (TTXr) in steps of 10 mV were used, followed by a 50-ms test pulse to 10 mV (TTXs) or 0 mV (TTXr) (Vh = −80 mV). For steady-state slow inactivation, 30-s pre-pulses from −120 mV to 0 mV in steps of 10 mV were used, followed by a 100-ms pulse to −120mV to remove fast inactivation, and then a 50-ms test pulse to 10 mV (TTXs) or 0 mV (TTXr) (Vh = −80 mV). For potassium current isolation, bath solution contained in (mM) 130 Choline-Cl, 5 KCL, 1 $MgCl_2$, 10 Glucose, 10 Hepes 10, pH 7.3 and 330 mOsm. Electrode internal solution was the same as the above for action potentials. K^+ currents were activated by 480-ms depolarizing voltage steps to potentials ranging between −35 and +45 mV in 10 mV increments preceded by a 2-second pre-pulse voltage step to either –100 mV (for whole current) or −10 mV (non-inactivating (IK) current only) (Gold et al 1996). The steady-state inactivation protocol consisted of a 2-second pre-pulse voltage step to potentials ranging between −110 and 0 mV followed by a depolarizing voltage step to +45 mV.

Recordings were analyzed using Clampfit 9 software. To obtain the midpoint of activation and steady-state fast and slow inactivation, peak currents were normalized to conductance (G). Subsequently, the data were plotted and fitted with a Boltzmann function: $G = Gmax/(1+ \exp[(V1/2 - V)/s])$, where Gmax is the fitted maximal conductance, V1/2 is the potential for half-maximal activation, and s is the slope factor. Data present mean ± SEM, and statistical significance ($p < 0.05$) was assessed by Student's t test or Analysis of Variance (ANOVA, one way) followed by Student-Newman-Keuls Post Hoc Test or Dunnet Post Hoc Test.

Results

We chose small-sized DRG cells with diameters in a relatively narrow range (20 to 30 μm; TTXs cells: 23.6 ± 1.4 pF, n = 59; TTXr cells, 22.0 ± 1.5 pF, n = 48) in order to have comparable passive cell membrane parameters. Under voltage-clamp configuration, each cell was first tested with 500 nM TTX to classify them into TTX-sensitive (TTXs) and TTX-resistant (TTXr) cells. TTXs cells were those cells whose voltage-evoked Na^+ currents were completely inhibited by 500 nM TTX (Fig. 1 right inset). TTXr cells were the cells whose voltage-evoked Na^+ currents retained at least 10% of total current in the presence of 500 nM TTX (Fig. 1 left inset). TTXr cells usually also expressed TTXs Na^+ currents of varying abundance as evidenced by the partial inhibition of Na^+ currents by TTX (Fig. 1 left inset).

Recordings were then switched to current-clamp configuration and effects of cooling temperatures on multiple action potential firing properties were tested. Figure 1 shows examples of the effects of cooling temperatures on action potential firing patterns in TTXr (Fig. 1A–E) and TTXs cells (Fig. 1F–H). At 24 °C, upon maintained membrane depolarization with current steps at 3X rheobase, TTXr cells (n = 37) showed several action

NIH-PA Author Manuscript

NIH-PA Author Manuscript

NIH-PA Author Manuscript

potential firing patterns, including phasic (n = 11, Fig. 1A), delayed (n = 4, Fig. 1B), irregular (n = 5, Fig. 1C), adaptive (n = 6, Fig. 1D), and tonic (n = 11, Fig. 1E). Twenty five (25) of them were tested with cooling temperatures of 15 °C, the same current steps increased firing frequency in 11 out 25 cells (11/25) identified as irregular (3/5), delayed (2/4), phasic (4/7), tonic (2/6), and adaptive (0/3) firing cells at 24 °C. The firing frequency of the remaining 14 cells tested were either maintained at the same level (n = 8) or reduced slightly (n = 6) in comparison with 24 °C. It was noticed that the types of cooling effects on TTXr cells were associated with the relative abundance of TTXr Na^+ currents. A total of 9 TTXr cells that responded to cooling with increased frequency showed a higher fraction of TTXr currents (77.4 ± 6.9 %, n = 9, see Fig. 1 left inset as an example of high fraction of TTXr currents). Out of the 14 cells that showed the maintained action potential firing at the cooling temperatures (see Fig. 1D&E), 11 had a relatively lower fraction of TTXr currents (30.2 ± 5.2 %, n = 11). Accordingly, we subdivided TTXr cells into high fraction TTXr Na^+ current group (TTXrh, TTXr currents > 55% of total Na^+ currents) and low fraction TTXr Na^+ current group (TTXrl, TTXr currents < 45% of total Na^+ currents). TTXs cells (n = 22) also showed tonic (n = 11, Fig. 1F), adaptive (n = 8, Fig. 1G), and phasic (n = 3, Fig. 1H) at 24 °C, but other firing pattern was not encountered. In sharp contrast to TTXr cells, cooling temperatures of 15 °C always converted multiple action potential firing to a single all-or-none firing (n = 12) either with or without subsequent aborted potentials (Fig. 1F–H).

A series of temperatures at 29, 24, 15, and 10 °C were tested on TTXrh cells. At 15 °C and 10 °C, action potential frequency was much higher than that of 29 °C and 24 °C at different current steps (Fig. 2A, 2D left panel). For example, at a 4-s current pulse of 0.09 nA, action potential numbers were significantly higher at 15 °C and 10 °C (8.3 ± 1.7, n = 9 and 9.0 ± 2.1, n = 9) than those at 24 °C and 29 °C (3.4 ± 0.8, n = 9 and 3.1 ± 2.0, n = 6, $P < 0.05$, Fig. 2D left panel). Cooling temperatures had little effect on action potential height in TTXrh cells (Fig. 2A&E). The height of the first and last action potentials elicited by a current pulse of 0.09 nA were not significantly different at any temperature from 29 °C to 10 °C (Fig. 2E). For example, action potential height were 63.3 ± 3.6 mV (first), and 61.6 ± 5.1 mV (last) at 24 °C (n= 7) and were 65.0 ± 2.0 mV (first), and 59.0 ± 2.2 mV (last) at 10 °C (n = 7). We examined membrane parameters of TTXrh cells (Supplementary Materials Table 1), including resting membrane potential (RMP), rheobase, action potential threshold, action potential width, action potential afterhyperpolarization (AHP) peak and amplitude, and input resistance. Except for resting membrane potential, which was not affected by cooling temperatures, all other parameters were altered by cooling temperatures. Rheobase lessened with decreasing temperatures. Also, action potential threshold increased (became less negative) at lower temperatures. Action potential width ($W_{1/2}$) increased with increasing cold, AHP amplitude decreased, and AHP peak became less negative with decreasing temperatures. Cell membrane input resistance was higher at lower temperatures.

For TTXrl cells, action potential firing properties were examined at 24 °C and 15 °C (Fig. 2B, 2D middle panel). Overall, these cells fired action potentials at a higher frequency than TTXrh cells at 24°C. For example, at a current step of 0.09 nA, TTXrl cells fired 18.8 ± 3.8 APs/4s (n = 11), while TTXrh cells only fired 3.4 ± 0.8 APs/4s (n = 9, $P < 0.05$). When action potential frequency of TTXrl cells at 24 and 15 °C was compared, they were similar at lower current steps and the frequency became lower only at higher current injections (≥ 0.09 nA, Fig. 2D middle panel). As temperature lowered from 24 °C to 15 °C, TTXrl cell input resistance, action potential threshold, and action potential width increased significantly, making all membrane parameters of TTXrl cells similar to those of TTXrh cells at 15 °C (Supplementary Materials Table 1).

In sharp contrast to TTXr cells, cooling temperatures always suppressed firing of multiple action potentials in TTXs cells (Fig. 2C, 2D right panel). At 15 °C and 10 °C, only a single

NIH-PA Author Manuscript

NIH-PA Author Manuscript

NIH-PA Author Manuscript

all-or-none full sized action potential could be elicited, which sometimes was followed by several aborted potentials (Fig. 2C, 2D right panel). Action potential height was significantly reduced at cooling temperatures (Fig. 2E), indicating increased adaptation and failure of action potentials at cooling temperatures. The height of last action potentials (including aborted) elicited by a current pulse of 0.09 nA (600 ms), was different across temperatures (29°C, 24°C, 15°C, and 10°C). For example, final action potential height was 48.8 ± 5.3 mV at 29 °C (n = 8), 38.4 ± 4.6 mV at 24 °C (n = 12), 28.8 ± 4.0 mV at 15 °C (n = 7), and 26.6 ± 6.1 mV at 10°C (n = 5) ($P < 0.05$). Cooing temperatures increased action potential threshold (became more positive) and action potential width, and decreased AHP peak (less negative) (Supplementary Materials Table 1). When membrane parameters of TTXs cells are compared with TTXr cells at each temperature (Supplementary Materials Table 1), TTXs cells have significantly lower rheobase and much lower action potential threshold.

We determined voltage-dependent activation and inactivation of TTXs and TTXr Na^+ channels at cooling temperatures. Both TTXr and TTXs Na^+ current amplitudes were progressively reduced when temperatures lowered from 29 to 10 °C (Fig. 3 A&B). When compared to 29 °C, cold at 15 °C induced a right-shift in the voltage-dependence of activation of TTXs Na^+ conductance (Fig. 3C right panel), $V_{1/2} = -30.1 \pm 2.9$ mV vs. -20.7 ± 1.7 mV (n = 10, $P < 0.05$), respectively. In contrast, the same temperature change did not significantly shift the voltage-dependent activation of TTXr Na^+ channels, $V_{1/2} = -19.5 \pm 2.0$ mV and -16.5 ± 2.1 mV at 29 °C and 15 °C respectively (n = 10, $P > 0.05$, Fig. 3C). The inhibition at each cooling temperatures was much less severe for TTXr than TTXs Na^+ channels (Fig. 3B&C). The differential inhibition by cooling temperatures of TTXs and TTXs Na^+ channel currents were not due to steady state fast inactivation (Fig. 3D) since the steady state fast inactivation of TTXr Na^+ channel was almost identical at 29°C and 10°C and steady state fast inactivation of TTXs Na^+ channel was also very similar at the two temperatures (Fig. 3D). However, TTXr Na^+ channels underwent fast inactivation at more depolarized potentials ($V_{1/2}$: -33.4 ± 0.5 mV at 29 °C, -33.5 ± 0.5 mV at 10 °C, n = 6) and TTXs at more hyperpolarized membrane potentials ($V_{1/2}$: -59.6 ± 1.2 mV at 29 °C, -54.2 ± 2.5 mV at 10 °C, n = 6) (Fig. 3D). We examined the steady-state slow inactivation of TTXs and TTXr Na^+ channels (Fig. 3E&F). At 24 °C, steady state slow inactivation of both TTXr and TTXs Na^+ channels had similar $V_{1/2}$ (TTXr: -50.5 ± 1.0 mV, n = 6; TTXs: -50.5 ± 2.2 mV, n = 6). Cooling temperature at 10 °C did not significantly affect TTXr Na^+ channel slow inactivation ($V_{1/2} = -49.8 \pm 0.5$ mV, Fig. 3F) but shifted TTXs Na^+ channel slow inactivation to much more hyperpolarized potential with $V_{1/2}$ of -87.5 ± 2.1 mV (Fig. 3E). At 10 °C and resting membrane potentials near −50 mV, the fraction of remaining current was about 20% for TTXs Na^+ channels and about 60% for TTXr Na^+ channels.

The increases of action potential width and decreases of AHP amplitude suggested that membrane repolarization was hampered by cooling temperatures (Supplementary Materials Table 1). Since A-type K^+ currents (IA currents) play a significant role in membrane repolarization, we examined effects of cooling temperatures on IA currents in both TTXs and TTXr cells. For the voltage protocol used in this study, we encountered two types of IA currents, IAf (fast inactivating IA) and IAs (slow inactivating IA)(Fig. 4C). Most of cells had IAs either with or without IAf. Of 18 TTXr cells examined, 7 were IAs only, 7 were a mixture of IAs and IAf, and 4 were IAf only. Of 15 TTXs cells examined, 9 were IAs only, 4 were a mixture of IAs and IAf, and 2 were IAf only. In all these cells there was always a non-inactivating IK current (Fig. 4B). Figure 5 shows a comparison of the isolated IA and IK currents in TTXr (n = 8) and TTXs (n =8) cells. In the cells included in this study, the amplitude of IA was comparable between TTXs and TTXr cells (Fig. 5A&D). IK currents were also comparable between the two types of cells (Fig. 4B&E). In addition, there was no significant difference in the steady state inactivation of the total K^+ currents between TTXs and TTXr cells (Fig. 5C).

NIH-PA Author Manuscript

NIH-PA Author Manuscript

NIH-PA Author Manuscript

Since K^+ currents did not significantly differ between the two groups, TTXs and TTXr cells were combined to study the effects of temperature on IA currents (Fig. 6A&D). Maximum IA current (120 ± 13 pA/pF, n = 16) was obtained at 29 °C with an activating pulse of 45 mV. At 24 °C, IA had already been significantly reduced with 68% (82 ± 10 pA/pF, n = 13) peak current remaining and was further inhibited at temperatures of 15 °C and 10 °C with 26% (31 ± 5 pA/pF, n = 11) and 12% (14 ± 3 pA/pF, n = 11) current remaining respectively. In contrast, IK was only slightly reduced by cooling temperatures as even at 10 °C 82 % (55 ± 11 pA/pF, n = 7) of current still remained from maximum current obtained at 29 °C (67 ± 8 pA/pF, n = 10, P > 0.05, Fig. 6B&E). Steady-state inactivation protocol showed that inhibition of IA currents by cold was not due to a voltage-dependent slow inactivation since hyperpolarizing potentials were unable to remove the inhibition of IA currents by cold temperatures (Fig. 6C&F). For example, with pre-pulsing to negative potentials of -100 mV for 2s, an activating pulse of 45 mV at 10 °C resulted in just 32 % (55 ± 7 pA/pF, n = 11) of the maximum current obtained at 29 °C (170 ± 14 pA/pF, n = 16, Fig. 6C&F). Similar to cold temperatures, IA currents were selectively inhibited by 100 μM 4-AP by 46% (92 ± 26 pA/pF before and 164 ± 30 pA/pF after 100 μM 4-AP, n = 5) while IK currents were not affected (data not shown).

If the inhibition of IA currents accounted for the changes of the excitability and action potential firing patterns at cooling temperatures, pharmacological block of IA currents should mimic the effects of cooling temperatures. Therefore, we examined effects of 100 μM 4-AP, a concentration which selectively inhibited IA currents, on both TTXs and TTXr cells. Indeed, at 24 °C 4-AP increased action potential firing numbers of TTXr cells (Fig. 7A, 7C left panel). For example, at a 0.15 nA current step, action potential firing numbers were 4.4 ± 2.0 APs/4s before 4-AP and increased to 10.2 ± 2.8 APs/4s after 4-AP (n = 6, P < 0.05). Action potential height was not significantly affected by 4-AP in TTXr cells (Fig. 7D left panel). On the other hand, in TTXs cells, 4-AP converted high-frequency tonic firing into adaptive firing with a reduction of action potential firing numbers (Fig. 7B,7C right panel). For example, with a current pulse of 0.15 nA, action potential firing numbers were 14.2 ± 3.0 APs/600ms before 4-AP and decreased to 6.3 ± 2.6 APs/600 ms after 4-AP (n = 6, P < 0.05). Action potential height became progressively reduced by 4-AP in TTXs cells (Fig. 7B, 7D right panel). Similar to cooling temperatures, 4-AP increased action potential width, and decreased AHP peak and rheobase for both TTXs and TTXr cells (Supplementary Materials Table 2). It had little effect on resting membrane potentials, action potential threshold, and input resistance in both TTXs and TTXr cells.

Discussion

A novel finding of the present study is that cooling temperatures preferentially inhibited IA currents but not IK currents in both TTXs and TTXr cells. We found that IA currents were significantly reduced at 24 °C, severely inhibited at 15 °C, and almost completely abolished at 10 °C. Since IA currents play an important role in modulating the action potential shape, threshold, and the inter-spike interval in sensory neurons (Yoshimura et al. 1996; Yost 1999), it is conceivable that cold temperatures can have a significant impact on sensory impulses through the inhibition of IA currents. Several types of IA currents have been identified in both nociceptive and non-nociceptive DRG neurons (Gold et al 1996; Yoshimura et al 1996). In our small-sized TTXs and TTXr cells, most showed either IAs currents only or a mixture of IAs and IAf currents. The inhibition of IA currents by cooling temperatures was due to the inhibition of its activation because the inhibition occurred even at very negative potentials that prevented steady-state inactivation. We show that the inhibition of IA currents has differential effects on the excitability of TTXs and TTXr cells. This may be due to differences in interplays between IA currents and voltage-gated Na channels in these two types of cells (see below).

NIH-PA Author Manuscript

NIH-PA Author Manuscript

NIH-PA Author Manuscript

In our study, TTXs cells showed several different firing properties at 24 °C. Cooling temperatures changed action potential firing properties from multiple firing (tonic or adaptive) to severe adaptive and phasic firing at 15 °C and 10 °C respectively. We found that cooling temperatures shifted TTXs channel steady-state slow inactivation curve to more hyperpolarizing voltages, resulting in substantial slow inactivation near resting membrane potentials, a result consistent with a previous study in mice (Zimmermann et al 2007). At noxious cold temperatures of 15 and 10 °C, we showed that the remaining TTXs channels were still able to generate a single all-or-none action potential firing in our small-sized TTXs DRG neurons, a result different from the previous study using Nav1.8 knockout mice for TTXs DRG neurons. Since TTXs channels in Nav1.8 knockout mice DRG neurons and our rat DRG neurons were similar, the discrepancy may be due to other factors such as cell size differences and/or differences in input resistance of the cells used in the two studies. Although we showed that TTXs cells could fire first action potentials at noxious cold temperatures, the subsequent action potential firing was aborted partially or completely. The failure of subsequent action potential firing was most likely due to the reduction of TTXs channel availability following the first action potential firing. Almost all TTXs channels undergo voltage-dependent inactivation at the peak of an action potential (Blair & Bean 2002). Therefore, TTXs channel availability after an action potential firing is dependent on membrane repolarization, during which TTXs channels recover from inactivation (Hess & El Manira 2001). Membrane repolarization during an action potential in our TTXs cells was at least partially dependent on IA currents. By inhibition of IA, cooling temperatures impaired membrane repolarization after an action potential firing as is evidenced by the broadened TTXs action potentials and reduced AHP. The impaired membrane repolarization and the shift of voltage-dependent inactivation of TTXs channels together were likely the causes of aborted action potentials at noxious cold temperatures. Consistently, low concentrations of 4-AP, which inhibit IA currents in TTXs cells, also changed tonic firing to adaptive or phasic firing in these cells. Thus, non-nonciceptive neurons that express only TTXs channels can be effectively silenced at nociceptive cooling temperatures.

Unlike the situation in TTXs cells, neither steady-state slow inactivation nor fast inactivation of TTXr channels was significantly affected by cooling temperatures, a result consistent with a previous study in mouse DRG neurons (Zimmermann et al 2007). This result supported the idea that TTXr channels retained the ability to conduct sensory impulses under nociceptive cold temperatures (Zimmermann et al 2007). Thus, even though TTXr cells express both TTXs and TTXr channels and both channels can function under innocuous temperatures, only TTXr channels on these cells can support the conduction of sensory impulses under noxious cold temperatures. Unlike TTXs cells, multiple action potential firing was maintained and even facilitated at cooling temperatures in TTXr cells. Increases in membrane input resistance by cooling temperatures have been suggested to account for increased excitability of nociceptors (Zimmermann et al 2007). However, in our study IA current inhibitor 4-AP, which did not significantly affect membrane input resistance, increased action potential firing frequency, a result consistent with previous studies in nociceptive-like small-sized DRG neurons (Vydyanathan et al 2005). This result suggests that IA is another important factor of the facilitation of action potential firing at cooling temperatures in TTXr cells. TTXr cells in our study were found to express IA currents. IA currents in TTXr cells were inhibited significantly by cooling temperatures, which may account for the reduction of AHP and the action potential broadening by cooling temperatures in these cells. In TTXr cells, a large IA current would be turned on before the membrane potential reached action potential threshold because these cells had a much higher threshold for action potential firing. Thus, IA in TTXr cells serves as a brake to oppose membrane depolarization and limit action potential firing. Inhibition of IA by cooling temperatures would release the brake to allow faster membrane depolarization and facilitate TTXr action potential firing.

NIH-PA Author Manuscript

NIH-PA Author Manuscript

NIH-PA Author Manuscript

Supplementary Material

Refer to Web version on PubMed Central for supplementary material.

Acknowledgments

We thank J. Strong and A. MacDermott for comments on an earlier version of this manuscript. IS and JL contributed to experimental design, data acquisition and analysis. JGG contributed to experimental design, data analysis and interpretation. This work was supported by a NIH grant DE018661 to J.G.G.

References

Akopian AN, Sivilotti L, Wood JN. A tetrodotoxin-resistant voltage-gated sodium channel expressed by sensory neurons. Nature. 1996; 379:257–262. [PubMed: 8538791]

Blair NT, Bean BP. Roles of tetrodotoxin (TTX)-sensitive Na+ current, TTX-resistant Na+ current, and Ca2+ current in the action potentials of nociceptive sensory neurons. J Neurosci. 2002; 22:10277–10290. [PubMed: 12451128]

Chien LY, Cheng JK, Chu D, Cheng CF, Tsaur ML. Reduced expression of A-type potassium channels in primary sensory neurons induces mechanical hypersensitivity. J Neurosci. 2007; 27:9855–9865. [PubMed: 17855600]

Dib-Hajj SD, Cummins TR, Black JA, Waxman SG. Sodium channels in normal and pathological pain. Annu Rev Neurosci. 2010; 33:325–347. [PubMed: 20367448]

Fruhstorfer H, Hermanns M, Latzke L. The effects of thermal stimulation on clinical and experimental itch. Pain. 1986; 24:259–269. [PubMed: 3960572]

Gold MS, Shuster MJ, Levine JD. Characterization of six voltage-gated K+ currents in adult rat sensory neurons. J Neurophysiol. 1996; 75:2629–2646. [PubMed: 8793767]

Guedj D, Weinberger A. Effect of weather conditions on rheumatic patients. Ann Rheum Dis. 1990; 49:158–159. [PubMed: 2322026]

Hess D, El Manira A. Characterization of a high-voltage-activated IA current with a role in spike timing and locomotor pattern generation. Proc Natl Acad Sci U S A. 2001; 98:5276–5281. [PubMed: 11309504]

McAlindon T, Formica M, Schmid CH, Fletcher J. Changes in barometric pressure and ambient temperature influence osteoarthritis pain. Am J Med. 2007; 120:429–434. [PubMed: 17466654]

McKemy DD, Neuhausser WM, Julius D. Identification of a cold receptor reveals a general role for TRP channels in thermosensation. Nature. 2002; 416:52–58. [PubMed: 11882888]

Meeusen R, Lievens P. The use of cryotherapy in sports injuries. Sports Med. 1986; 3:398–414. [PubMed: 3538270]

Morin C, Bushnell MC. Temporal and qualitative properties of cold pain and heat pain: a psychophysical study. Pain. 1998; 74:67–73. [PubMed: 9514562]

Peier AM, Moqrich A, Hergarden AC, Reeve AJ, Andersson DA, et al. A TRP channel that senses cold stimuli and menthol. Cell. 2002; 108:705–715. [PubMed: 11893340]

Phillips JR, Matthews PB. Texture perception and afferent coding distorted by cooling the human ulnar nerve. J Neurosci. 1993; 13:2332–2341. [PubMed: 8501511]

Rasband MN, Park EW, Vanderah TW, Lai J, Porreca F, Trimmer JS. Distinct potassium channels on pain-sensing neurons. Proc Natl Acad Sci U S A. 2001; 98:13373–13378. [PubMed: 11698689]

Sarria I, Gu J. Menthol response and adaptation in nociceptive-like and nonnociceptive-like neurons: role of protein kinases. Mol Pain. 2010; 6:47. [PubMed: 20727164]

Sato J. Weather change and pain: a behavioral animal study of the influences of simulated meteorological changes on chronic pain. Int J Biometeorol. 2003; 47:55–61. [PubMed: 12647091]

Sculptoreanu A, Yoshimura N, de Groat WC. KW-7158 [(2S)-(+)-3,3,3-trifluoro-2-hydroxy-2-methyl-N-(5,5,10-trioxo-4,10-dihydro thieno[3,2-c][1]benzothiepin-9-yl)propanamide] enhances A-type K + currents in neurons of the dorsal root ganglion of the adult rat. J Pharmacol Exp Ther. 2004; 310:159–168. [PubMed: 15010502]

NIH-PA Author Manuscript

NIH-PA Author Manuscript

NIH-PA Author Manuscript

Tan ZY, Donnelly DF, LaMotte RH. Effects of a chronic compression of the dorsal root ganglion on voltage-gated Na+ and K+ currents in cutaneous afferent neurons. J Neurophysiol. 2006; 95:1115–1123. [PubMed: 16424456]

Tsuzuki K, Xing H, Ling J, Gu JG. Menthol-induced Ca2+ release from presynaptic Ca2+ stores potentiates sensory synaptic transmission. J Neurosci. 2004; 24:762–771. [PubMed: 14736862]

von Mackensen S, Hoeppe P, Maarouf A, Tourigny P, Nowak D. Prevalence of weather sensitivity in Germany and Canada. Int J Biometeorol. 2005; 49:156–166. [PubMed: 15338386]

Vydyanathan A, Wu ZZ, Chen SR, Pan HL. A-type voltage-gated K+ currents influence firing properties of isolectin B4-positive but not isolectin B4-negative primary sensory neurons. J Neurophysiol. 2005; 93:3401–3349. [PubMed: 15647393]

Yoshimura N, White G, Weight FF, de Groat WC. Different types of Na+ and A-type K+ currents in dorsal root ganglion neurones innervating the rat urinary bladder. J Physiol. 1996; 494(Pt 1):1–16. [PubMed: 8814602]

Zimmermann K, Leffler A, Babes A, Cendan CM, Carr RW, et al. Sensory neuron sodium channel Nav1.8 is essential for pain at low temperatures. Nature. 2007; 447:855–858. [PubMed: 17568746]

NIH-PA Author Manuscript
NIH-PA Author Manuscript
NIH-PA Author Manuscript

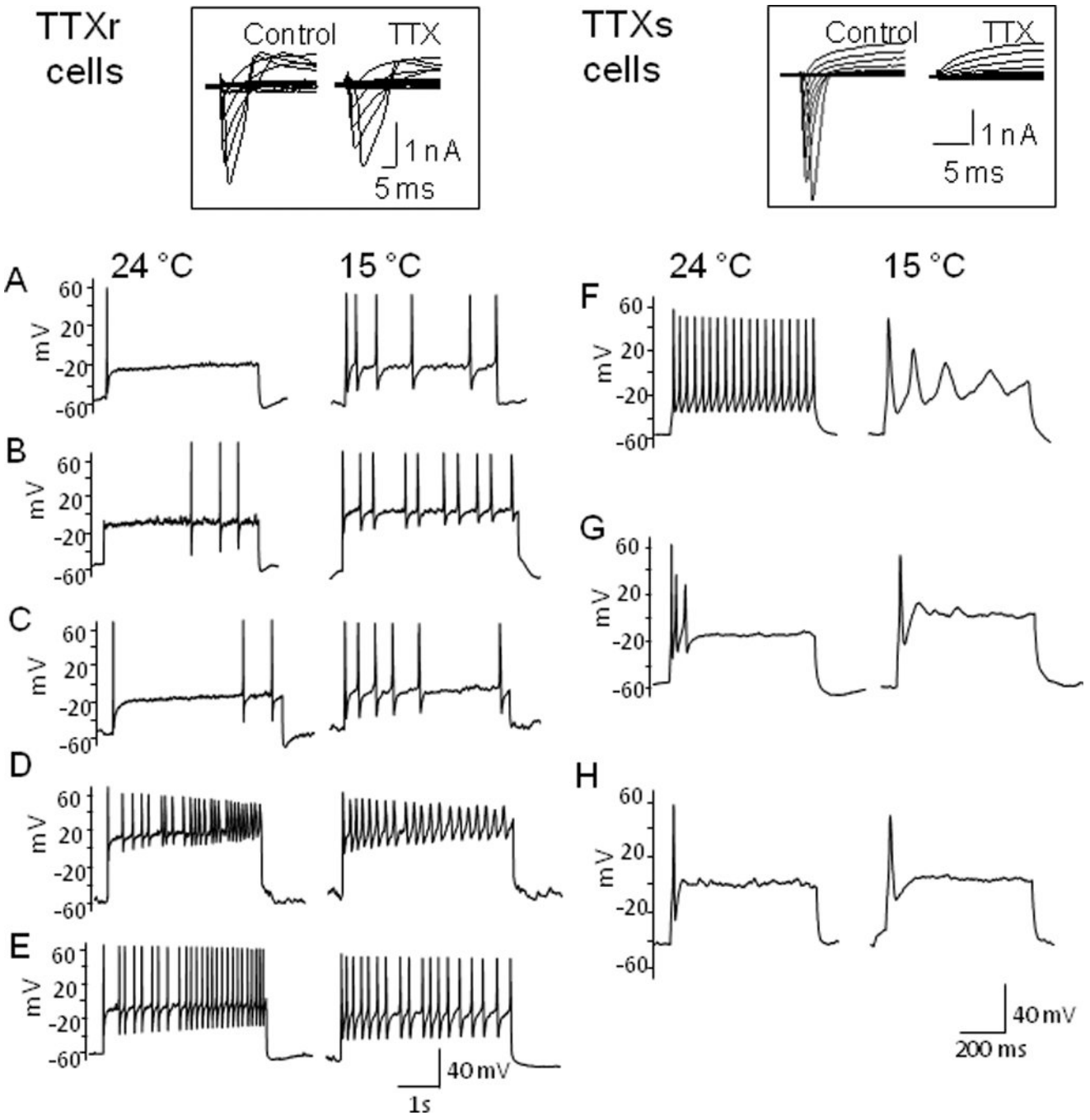

Fig. 1. Cooling temperatures differentially affect action potential firing patterns in TTXr and TTXs small DRG neurons

(**A–E**) Representative traces show action potential firing patterns of TTXr cells at 24 and 15 °C. At 24 °C, several action potential firing patterns were encountered. The same current step at 15 °C either increased spike numbers (**A–C**) or maintained multiple action potential firing patterns in TTXr neurons. Inset shows an example of a neuron with a high fraction of TTXr Na^+ currents as tested with 500 nM TTX. (**F-H**) Representative traces show action potential firing patterns of TTX-sensitive (TTXs) at 24 and 15 °C. At 24 °C, several action potential firing patterns were encountered. Cooling temperature of 15 °C allowed only single but not multiple full action potentials in TTXs neurons. Inset shows an example of a neuron

NIH-PA Author Manuscript

NIH-PA Author Manuscript

NIH-PA Author Manuscript

with only TTXs Na^+ currents. Each cell was first pre-identified as a TTXr cell or a TTXs cell by testing TTX-sensitivity of Na^+ currents under voltage-clamp configuration. Recordings were then switched to current-clamp configuration and current pulses at 3x rheobase were injected into the cells.

NIH-PA Author Manuscript
NIH-PA Author Manuscript
NIH-PA Author Manuscript

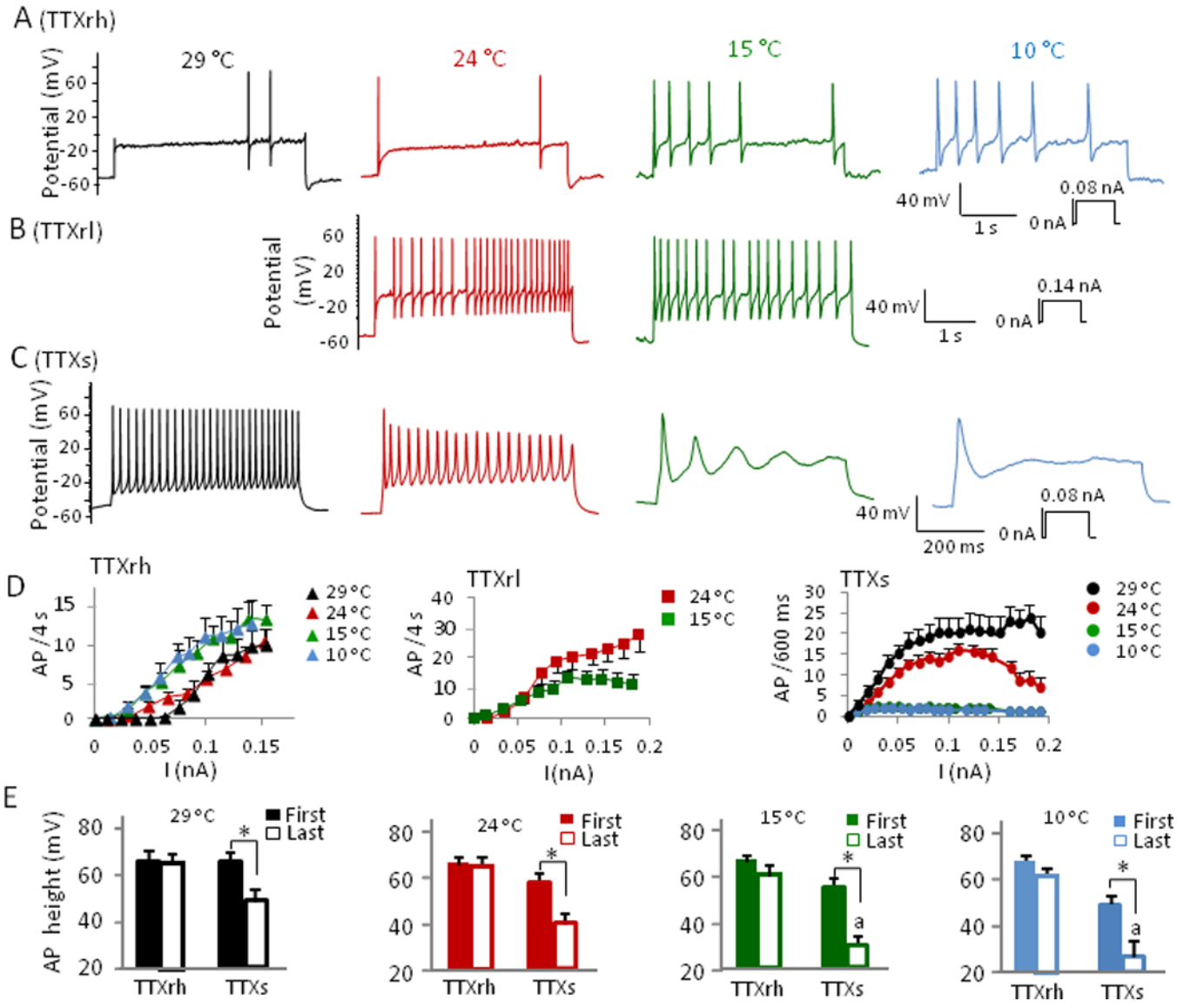

Fig. 2. Analysis of cooling effects on action potential firing of TTXrh, TTXrl, and TTXs small DRG neurons

(**A-C**) Representative traces show effect of cooling temperatures on action potential firing in DRG neurons pre-identified as TTXrh (**A**), TTXrl (**B**), and TTXs cells (**C**). Cells were given a series of current pulses at 29 °C, 24 °C, 15 °C, and 10 °C. TTXrh: cells had high abundance of TTXr Na^+ channels; TTXrl: cells had relatively low abundance of TTXr Na^+ channels. (**D**) Summary of action potential (AP) firing frequency at different temperatures for TTXrh cells (left panel of D, n = 6 to 9), TTXrl cells (middle panel of D, 24 °C, n = 11), and TTXs cells (right panel of D, 29 °C, n = 8 to 12). Significant difference ($P < 0.05$) is not indicated in the figures for clarity. Action potential numbers are significantly higher at 15 °C and 10 °C than those at 24 °C and 29 °C at current steps of ≥ 0.05 nA for TTXrh group, steps of ≥ 0.09 nA for TTXrl, and steps of ≥ 0.02 nA for TTXs group. (**E**) Summary of the effect of temperatures on action potential height for TTXrh and TTXs cells at different temperatures, n is same as in (**D**) for both groups. First and last action potentials (including abortive) were selected from the lowest current step that yielded maximum AP frequency in each cell. Data represent mean ± SEM. * $P < 0.05$, a = abortive action potential.

NIH-PA Author Manuscript
NIH-PA Author Manuscript
NIH-PA Author Manuscript

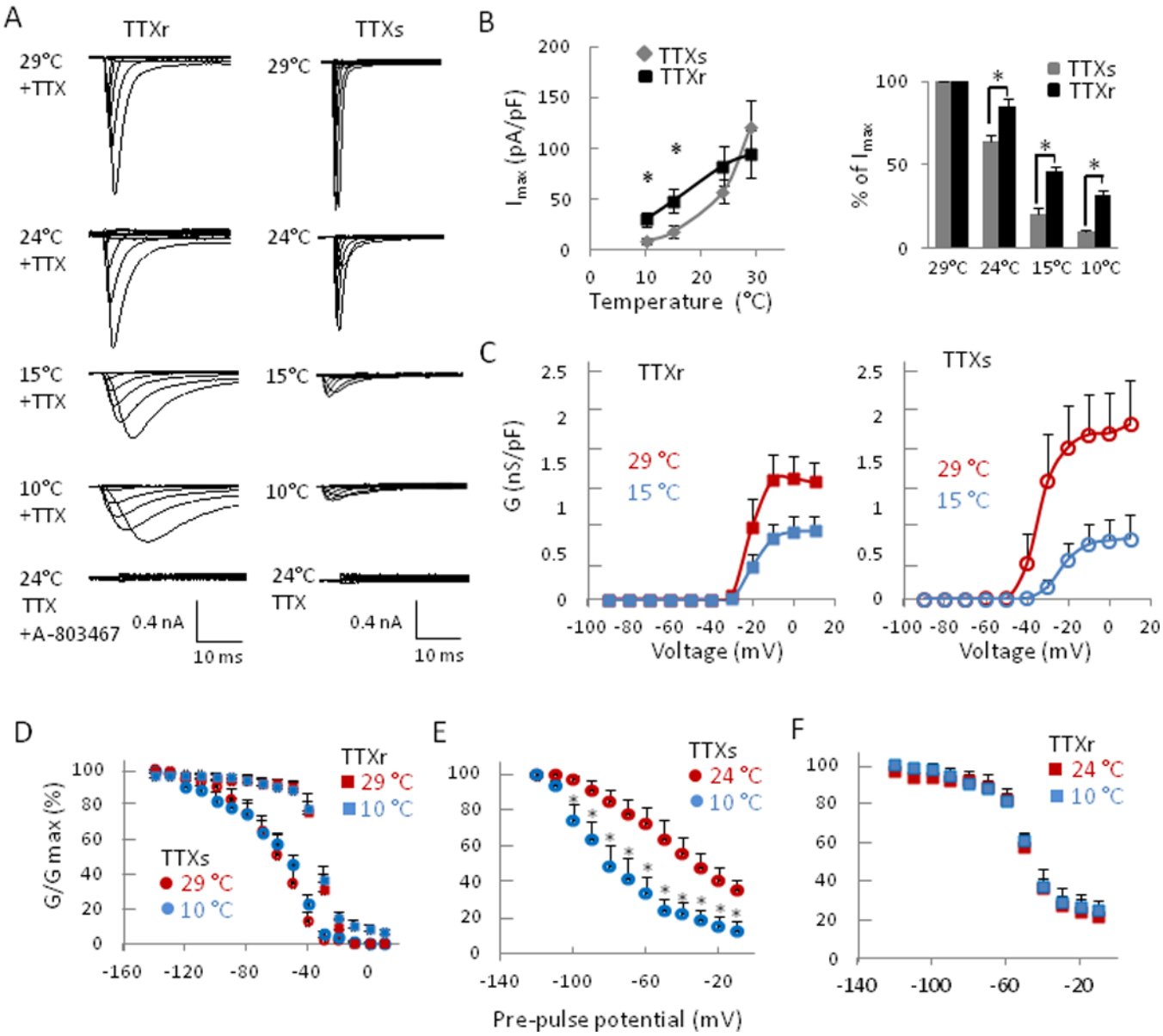

Fig. 3. Cooling temperatures differentially affect TTXs and TTXr currents in small DRG neurons

(**A**) Representative traces of TTXr (left) and TTXs (right) Na^+ currents in DRG neurons recorded at 29, 24, 15 and 10 °C. Cells were held at −80 mV and Na^+ channel currents were activated by 500-ms test pulses from −90 to +10 mV in steps of 10 mV. TTXr Na^+ currents were isolated by including 500 nM TTX in the bath solution. A-803467, a Na_v 1.8 channel specific blocker (100 μM), completely blocked TTXr Na^+ channel currents at 24 °C. (**B**) Summary of maximum currents (I_{max}, left panel) at different temperatures in TTXs (n = 10) and TTXr cells (n = 10), and percentage of maximum current at different temperatures relative to I_{max} at 29 °C (right panel, n = 10). (**C**) Voltage-dependent activation of TTXr (n = 10, left panel) and TTXs (n = 10, right panel) at 29 °C and 15 °C. Vh = −80 mV. (**D**) Summary of steady-state fast inactivation of TTXs (circles, n = 6) and TTXr (squares, n = 6) Na^+ currents in DRG neurons. Experiments were performed at 29 °C (red symbols) and 10 °C (blue symbols). (**E-F**) Summary of steady-state slow inactivation of TTXs (**D**, n = 6) and

NIH-PA Author Manuscript

NIH-PA Author Manuscript

NIH-PA Author Manuscript

TTXr (**E**, n = 6) Na^+ currents in DRG neurons. Experiments were performed at 24 °C (red symbols) and 10 °C (blue symbols). Data represent Mean ± SEM. *P < 0.05, 10 °C vs. 24 °C.

NIH-PA Author Manuscript
NIH-PA Author Manuscript
NIH-PA Author Manuscript

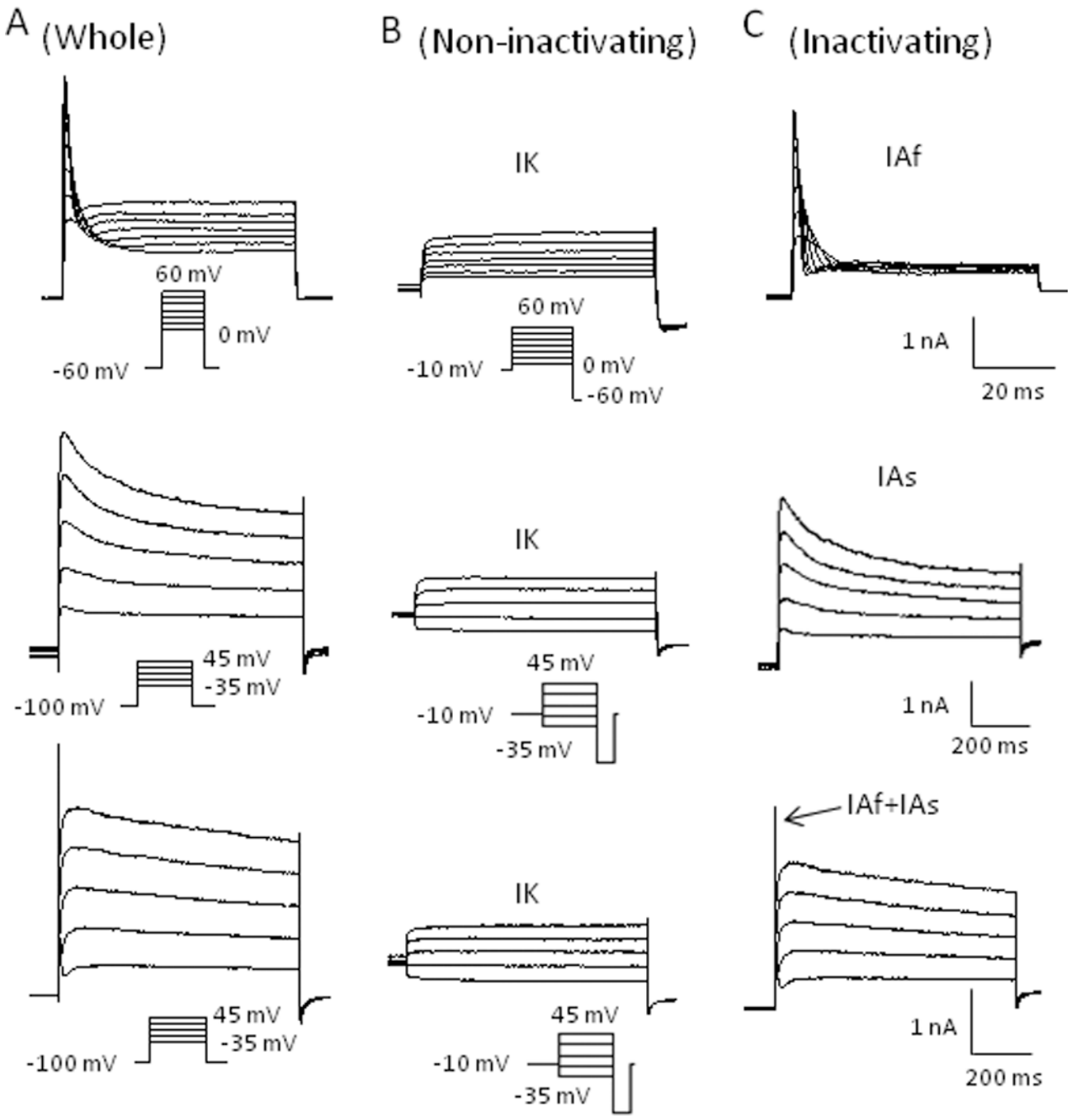

Fig. 4. Isolation of non-inactivating and inactivating voltage-gated K^+ currents in small DRG neurons

(**A**) Representative traces of whole outward currents from three separated cells evoked by voltage steps (shown below the traces) from a 2-second pre-potential of −60 mV (top) or −100 mV (middle and bottom). (**B**) Same activation steps as in **A**, but preceded by a 2-second pre-pulse to −10 mV to remove inactivating current component, which isolated non-inactivating K^+ currents (IK currents). (**C**) Subtraction of non-inactivating currents from whole-currents revealed two types of inactivating K^+ currents (IA currents): fast inactivating (IAf) (top) and slow inactivating (IAs) currents (middle) in two separate DRG neurons. The bottom panel shows the mixture of both IAf and IAs currents in a single DRG neuron.

NIH-PA Author Manuscript
NIH-PA Author Manuscript
NIH-PA Author Manuscript

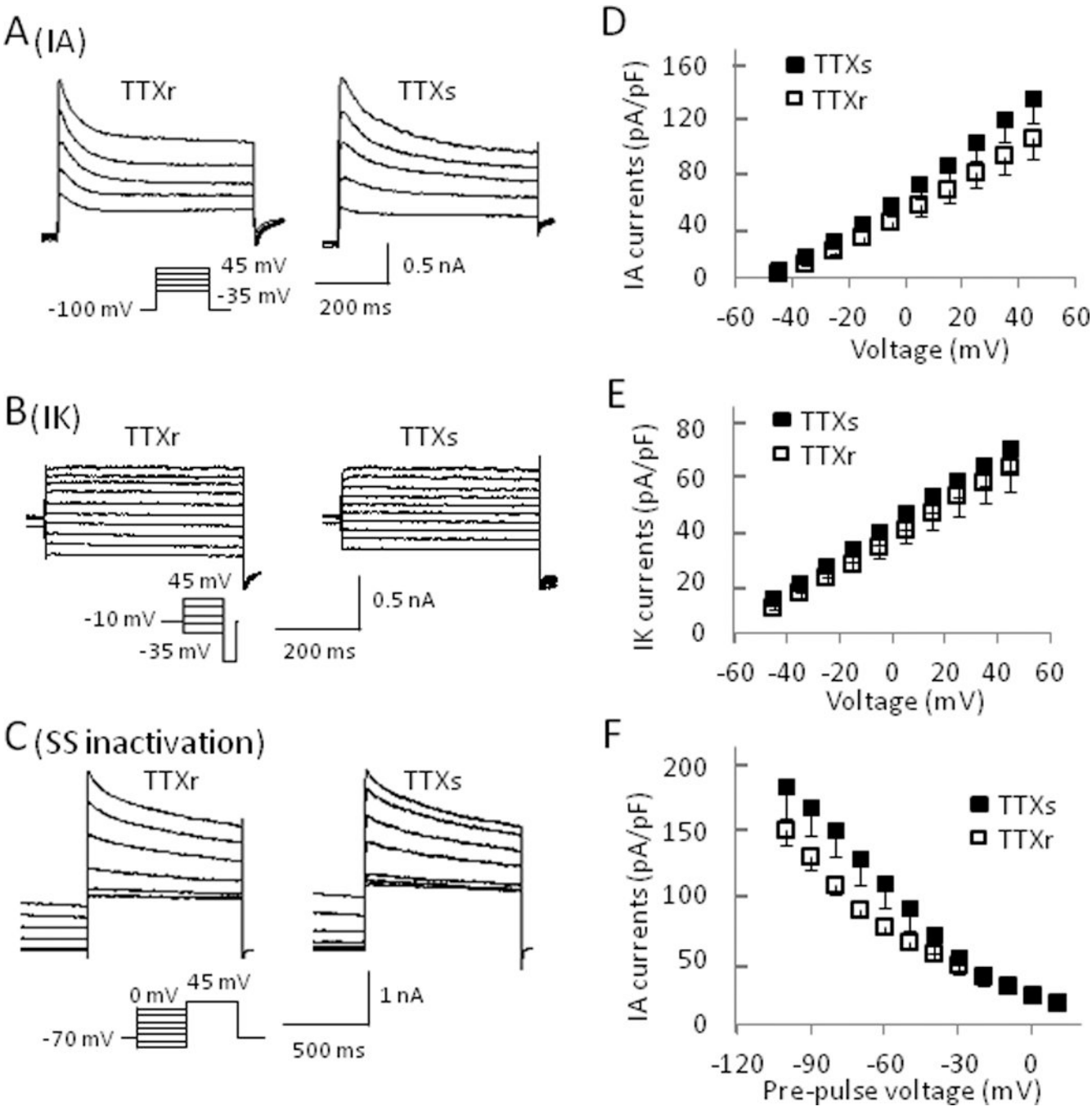

Fig. 5. Comparison of voltage-gated K^+ currents in TTXr and TTXs small DRG neurons

(**A&B**) Representative traces of IA (**A**) and IK (**B**) currents from a TTXr (left) and a TTXs (right) DRG neuron. (**C**) Traces showing the steady state inactivation of whole K^+ currents in a TTXr (left) and a TTXs cell (right). Steady state inactivation protocol consisted of a 2-second pre-pulse voltage step to potentials ranging between −110 and 0 mV followed by a depolarizing step to +45 mV. (**D&E**) Summary of peak IA (**D**) and IK (**E**) currents plotted versus activating potentials from both TTXr and TTXs cells. (**F)** Summary of peak currents from TTXr and TTXs cells plotted vs. pre-pulse potentials from the steady state inactivation

protocol. Current amplitude was normalized by cell capacitance. TTXr cells: n = 8, TTXs cells: n = 8.

NIH-PA Author Manuscript
NIH-PA Author Manuscript
NIH-PA Author Manuscript

NIH-PA Author Manuscript
NIH-PA Author Manuscript
NIH-PA Author Manuscript

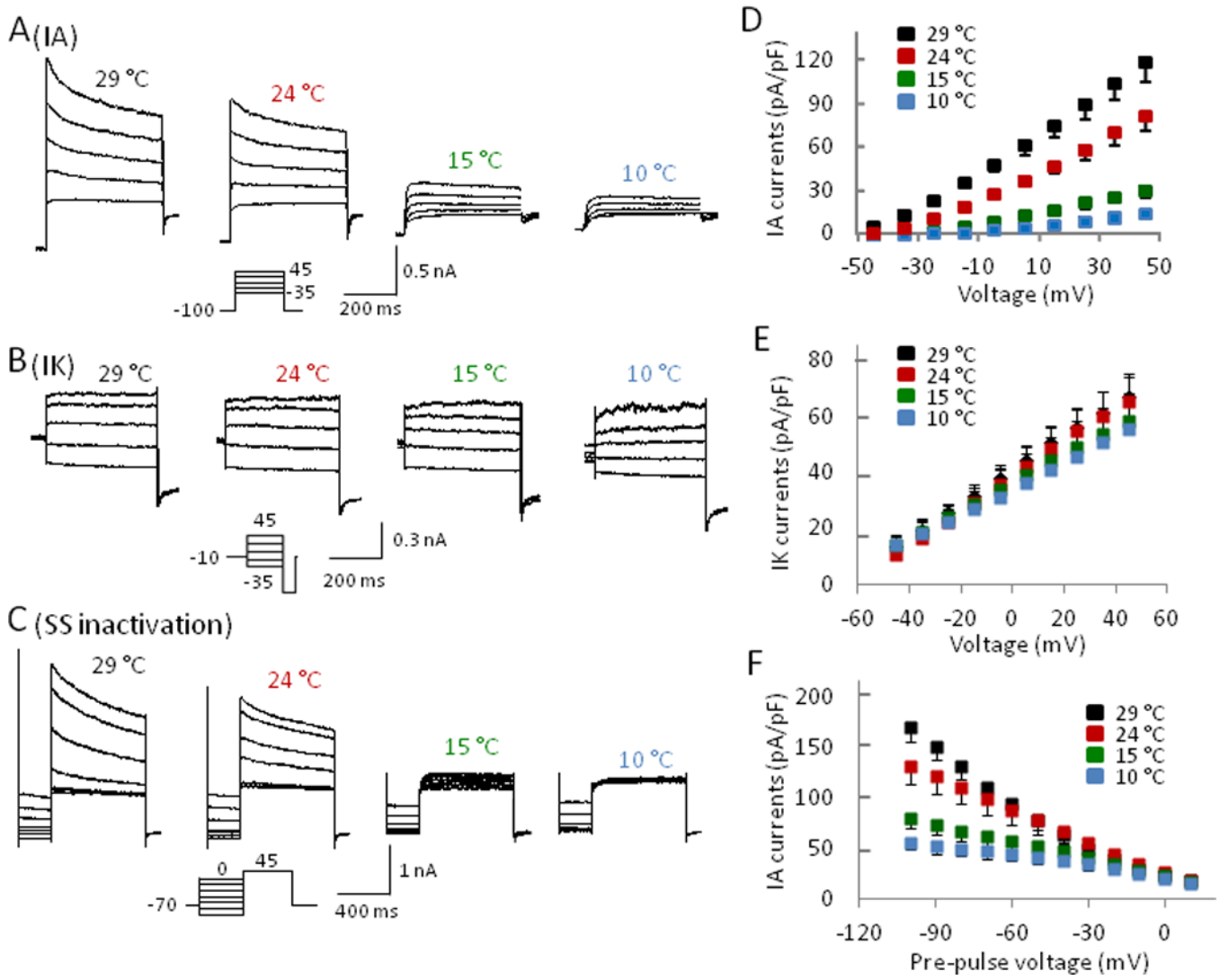

Fig. 6. Cooling temperatures inhibit the activation of IA currents in small DRG neurons

(**A–C**) Representative traces obtained from a neuron showing activation of isolated IA (**A**) and IK (**B**) currents as well as steady state inactivation of whole K^+ currents (**C**) at 29°C, 24°C, 15°C, and 10°C. (**D–F**) Summary of maximum IA (**D**) and IK (**E**) currents and steady state inactivation of whole K^+ currents (**F**) at 29°C (n = 16), 24 °C (n = 13), 15 °C (n = 11), and 10°C (n = 11).

NIH-PA Author Manuscript
NIH-PA Author Manuscript
NIH-PA Author Manuscript

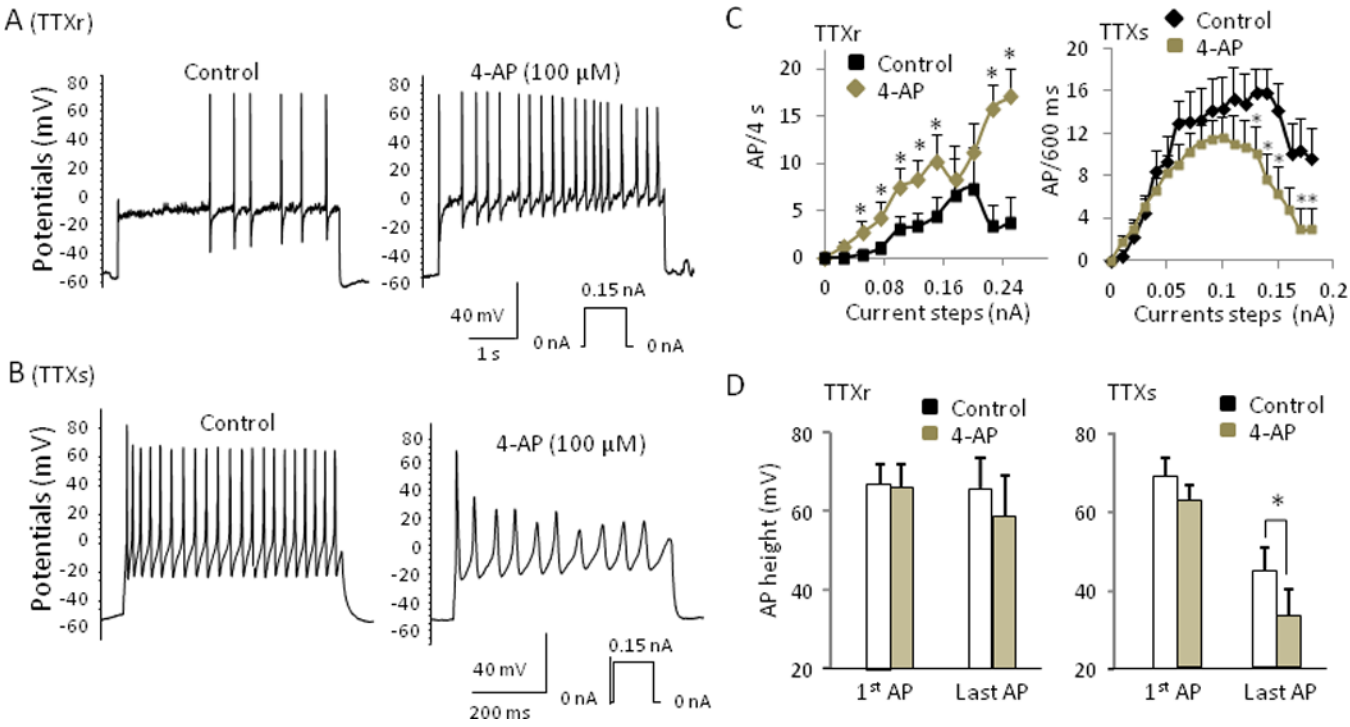

Fig. 7. 4-AP enhances action potential firing in TTXr, but not in TTXs small DRG neurons

(**A&B**) Sample traces showing action potential firing of a TTXr (**A**) and a TTXs (**B**) cell before (left) and after (right) exposure to 100 µM 4-AP. (**C**) Action potential firing frequency of TTXr (left) and TTXs (right) cells before and after 100 µM 4-AP. (**D**) Effect of 4-AP on action potential height of TTXr (left, n = 6) and TTXs (right, n = 6). Data are mean ± SEM, * P < 0.05, 4-AP vs. control.